

## Supplementary Information

### Table of Contents

#### 1. General experimental procedures

Characterization

#### 2. Synthesis

**Scheme S1.** The synthetic routes of PTZ-2BP and PTZ-2FBP.

#### 3. Figures and Tables

**Fig. S1** UV and PL spectra of PTZ-2BP and PTZ-2FBP in THF solution.

**Fig. S2** PL decay curves of PTZ-2BP and PTZ-2FBP in THF solution.

**Fig. S3** ML spectra of PTZ-2BP under continuous mechanical stimulus within 30 s.

**Fig. S4** The (a) PL decay and (b) long-lived PL decay of PTZ-2BP in different states.

**Fig. S5** (a) Normalized PL spectra of PTZ-2FBP in original (-o) and ground (-g) states; (b) PL decay of PTZ-2FBP in original (-o) and ground (-g) states.

**Fig. S6** The delayed PL spectra of PTZ-2FBP in original (-o) and ground (-g) states.

**Fig. S7** The phosphorescence spectra of PTZ-2BP and PTZ-2FBP in the as-prepared state at 77 K.

**Fig. S8** The nanoindentation test of a typical load versus displacement (P-h) curve.

**Fig. S9** The molecular packing in the crystals of PTZ-2BP and PTZ-2FBP.

**Fig. S10** The calculated intramolecular noncovalent interactions (NCI) based on reduced density gradient (RDG) in the molecular dimer derived from the unit cell of PTZ-2BP or PTZ-2FBP.

**Fig. S11** The calculated conformations based on PTZ-2FBP.

**Fig. S12** The electrochemical cyclic voltammetry curves of PTZ-2BP and PTZ-2FBP.

**Fig. S13** The HOMO and LUMO of the single molecules in the PTZ-2BP and PTZ-2FBP calculated at B3LYP/6-31G(d, p) level.

**Fig. S14** The HOMO and LUMO of the dimers in the PTZ-2BP and PTZ-2FBP calculated at B3LYP/6-31G(d, p) level.

**Fig. S15** The lowest singlet ( $S_1$ ) and triplet ( $T_n$ ) states of a PTZ-2BP monomer and two PTZ-2FBP monomers, respectively obtained by TD-DFT calculations based on the single crystal structure data.

**Fig. S16** The lowest singlet ( $S_1$ ) and triplet ( $T_n$ ) states of a PTZ-2BP dimer and two PTZ-2FBP dimers, respectively obtained by TD-DFT calculations based on the single crystal structure data.

**Fig. S17** The Differential Scanning Calorimetry (DSC) curves of PTZ-2BP and PTZ-2FBP.

**Fig. S18** The Thermogravimetric analysis (TGA) curves of PTZ-2BP and PTZ-2FBP.

**Fig. S19** The High Performance Liquid Chromatography (HPLC) of PTZ-2BP and PTZ-2FBP.

**Table S1** The photophysical data of PTZ-2BP and PTZ-2FBP in THF solution.

**Table S2** ML wavelength of PTZ-2BP under continuous mechanical grinding within 30 s.

**Table S3** Optical properties of PTZ-2FBP in *o* and *g* state.

**Table S4** Structure data of crystals PTZ-2BP and PTZ-2FBP.

**Table S5-7** Summarization of intermolecular interactions in the molecular dimer derived from the unit cell of PTZ-2BP and PTZ-2FBP.

**Table S8-9** Singlet and triplet excited state transition configurations of PTZ-2BP monomer/dimer and PTZ-2FBP monomers/dimers revealed by TD-DFT calculations.

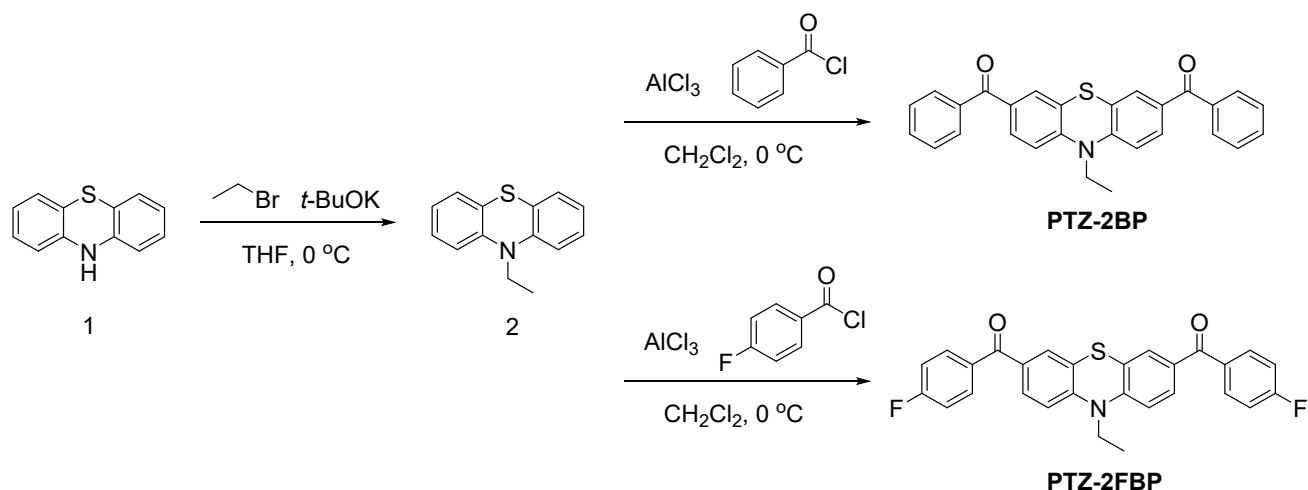
#### 4. Structure Information

**Fig. S20-S24**  $^1\text{H}$  NMR and  $^{13}\text{C}$  NMR spectra of PTZ derivatives conducted in  $\text{CDCl}_3$ .

## 1. General experimental procedures

**Characterization:**  $^1\text{H}$  and  $^{13}\text{C}$  NMR spectra were recorded on a 400 MHz Varian Mercury, using  $\text{CDCl}_3$  as the solvent. High resolution mass spectrometry (HRMS) was measured by an Agilent 7250 & JEOL-JMS-T100LP AccuTOF mass spectrophotometer. High performance liquid chromatography (HPLC) was performed by a Shimadzu LC-20AD (85 bar, 1 mL/min, 7%  $\text{H}_2\text{O}$  93% MeOH). PL spectra were recorded by a Hitachi F-4600 fluorescence spectrophotometer. The ML spectra were measured on a spectrometer of Acton SP2750 with CCD (SPEC-10, Princeton) as a power detector. Absolute photoluminescence quantum yield (PLQY) and luminescence decay were recorded by an Edinburgh FLS920 spectrometer. The powder X-ray diffraction patterns were measured on Panalytical X'pert powder at 25 °C at 40 kV and 40 mA at a scan rate of  $10^\circ$  (2 $\theta$ )/min (scan range: 5-60°). The single-crystal X-ray diffraction data were recorded by a Bruker D8 Venture diffractometer. The CCDC numbers of PTZ-2FBP and PTZ-2BP are 2391557 and 2391558 respectively. Differential scanning calorimetry were performed on TA Q20 instrument from room temperature to 250 °C at a heating rate of 10 °C/min under nitrogen. The Gaussian 09 program was utilized to perform the TD-DFT calculations. The ground state ( $S_0$ ) geometry was obtained from the single crystal structure and no further geometry optimization was conducted in order to maintain the specific molecular configuration and corresponding intermolecular locations.

## 2. Synthesis



**Scheme S1.** The synthetic routes of PTZ-2BP and PTZ-2FBP.

**Compound 2:** To a Schlenk flask was added Phenothiazine (1.99 g, 10 mmol), potassium tert-butoxide (1.68 g, 15 mmol) and THF (30 mL). The resultant solution was stirred under nitrogen atmosphere at 0 °C for 20 min. Then ethyl bromide (1.12 mL, 15 mmol) was added at 0 °C and stirred for another 12 h. After the reaction completed, the mixture was cooled to room temperature and quenched with water, then

extracted by dichloromethane. The combined organic extracts were dried over anhydrous  $\text{Na}_2\text{SO}_4$  and concentrated by rotary evaporation to afford a crude product. The crude product was purified by column chromatography using petroleum ether as eluent to give the pure compound 2 as a white solid (1.71 g, 75%).  $^1\text{H}$  NMR (400 MHz,  $\text{CDCl}_3$ ,  $\delta$ ): 7.17-7.13 (m, 4H, Ar-H), 6.90-6.86 (m, 4H, Ar-H), 3.93 (s, 2H,  $-\text{CH}_2$ ), 1.56-1.41 (m, 3H,  $-\text{CH}_3$ ). MS (EI),  $m/z$ : 227.07, calcd for  $\text{C}_{14}\text{H}_{13}\text{NS}$ : 227.08.

**PTZ-2BP**: Under a nitrogen atmosphere, compound 2 (1.82 g, 8.0 mmol) and  $\text{AlCl}_3$  (2.35 g, 17.6 mmol) were dissolved in anhydrous dichloromethane (DCM) (20 mL). The reaction mixture was stirred at 0 °C for 30 min, then a solution of benzoyl chloride (2.03 mL, 17.6 mmol) in anhydrous DCM (20 mL) was slowly added at 0 °C. After stirred at room temperature for 6 h, the reaction was quenched with water and extracted with dichloromethane. The organic layer was dried over anhydrous  $\text{Na}_2\text{SO}_4$  and concentrated in vacuum. The crude product was purified by column chromatography (eluent: petroleum ether/dichloromethane = 1/2) to give the pure compound of PTZ-2BP as a yellow solid (2.09 g, 60%).  $^1\text{H}$  NMR (400 MHz,  $\text{CDCl}_3$ ,  $\delta$ ): 7.76-7.74 (d,  $J$  = 8 Hz, 4H, Ar-H), 7.67-7.64 (m, 2H, Ar-H), 7.60-7.56 (m, 4H, Ar-H), 7.50-7.46 (m, 4H, Ar-H), 6.94-6.92 (d,  $J$  = 8 Hz, 2H,  $-\text{CH}_2$ ), 1.63-1.48 (s, 3H,  $-\text{CH}_3$ ).  $^{13}\text{C}$  NMR (100 MHz,  $\text{CDCl}_3$ ,  $\delta$ ): 194.59, 147.30, 137.82, 132.26, 132.17, 130.57, 129.67, 129.38, 128.33, 123.08, 114.44, 42.73, 12.77. HRMS ( $\text{ESI}^+$ ),  $m/z$ : 436.13, calcd for  $\text{C}_{28}\text{H}_{21}\text{NO}_2\text{S}$ : 435.12. [CCDC 2391558]

**PTZ-2FBP**: Similar procedure to that of **PTZ-2BP**. Compound 2 (1.82 g, 8.0 mmol) and  $\text{AlCl}_3$  (2.35 g, 17.6 mmol) were dissolved in anhydrous dichloromethane (DCM) (20 mL). A solution of 4-fluorobenzoyl chloride (2.08 mL, 17.6 mmol) in anhydrous DCM (20 mL). The crude product was purified by column chromatography (eluent: petroleum ether/dichloromethane = 1/2) to give the pure compound of PTZ-2FBP as an orange solid (2.45 g, 65%).  $^1\text{H}$  NMR (400 MHz,  $\text{CDCl}_3$ ,  $\delta$ ): 7.81-7.77 (m, 4H, Ar-H), 7.63-7.61 (d,  $J$  = 8 Hz, 2H, Ar-H), 7.53 (s, 2H, Ar-H), 7.18-7.14 (m, 4H, Ar-H), 6.95-6.93 (d,  $J$  = 8 Hz, 2H, Ar-H), 4.06-4.01 (m, 2H,  $-\text{CH}_2$ ), 1.63-1.48 (m, 3H,  $-\text{CH}_3$ ).  $^{13}\text{C}$  NMR (100 MHz,  $\text{CDCl}_3$ ,  $\delta$ ): 193.11, 166.49, 163.97, 147.31, 133.99, 133.96, 132.30, 132.21, 132.17, 130.43, 129.20, 123.16, 115.62, 115.40, 114.49, 42.75, 12.75. HRMS ( $\text{ESI}^+$ ),  $m/z$ : 472.11, calcd for  $\text{C}_{28}\text{H}_{19}\text{F}_2\text{NO}_2\text{S}$ : 471.11. [CCDC 2391557]

### 3. Figures and Tables

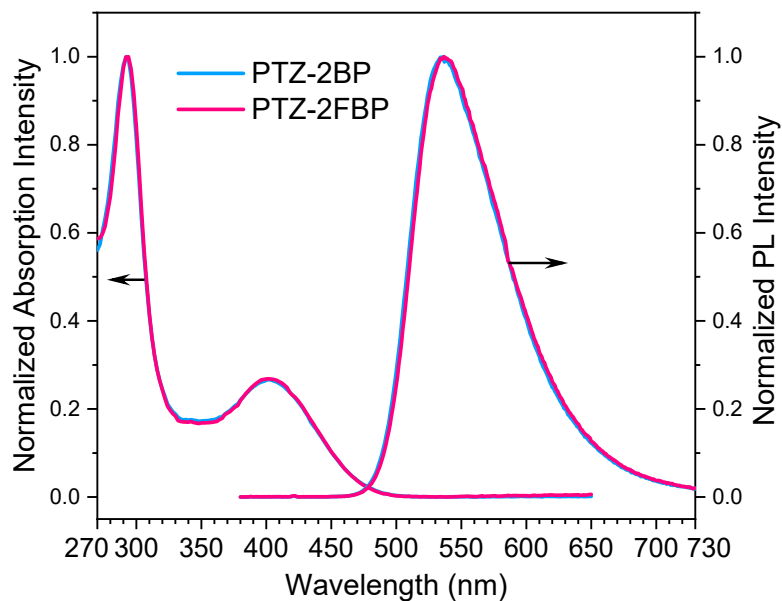


**Figure S1.** UV and PL spectra of PTZ-2BP and PTZ-2FBP in THF solution. ( $c = 10^{-5}$  M)

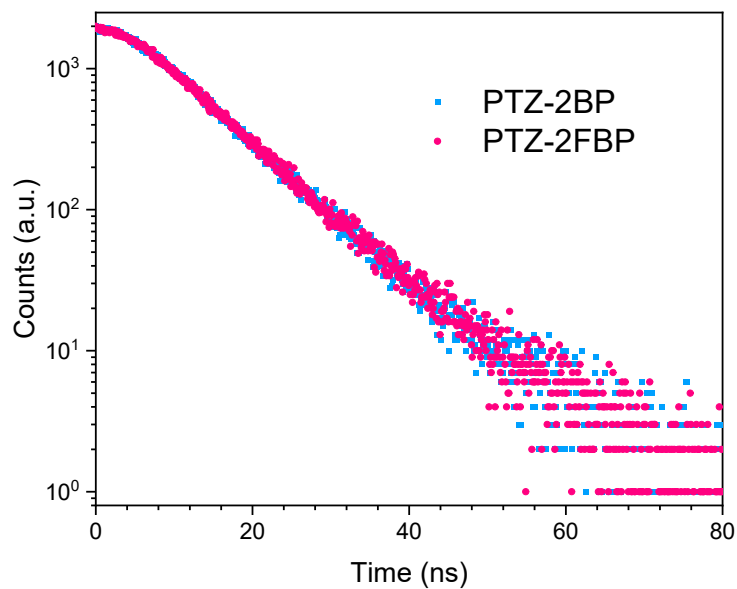


**Figure S2.** PL decay curves of PTZ-2BP and PTZ-2FBP in THF solution. ( $c = 10^{-5}$  M,  $\lambda_{\text{ex}} = 375$  nm)

**Table S1.** The photophysical data of PTZ-2BP and PTZ-2FBP in THF solution. ( $c = 10^{-5}$  M)

Compound	$\lambda_{\text{abs}}$ (nm)	$\lambda_{\text{em}}$ (nm)	$\tau$ (ns)	$\Phi$ (%)
PTZ-2BP	292,402	536	9.50	71.49
PTZ-2FBP	294,400	537	9.47	81.52

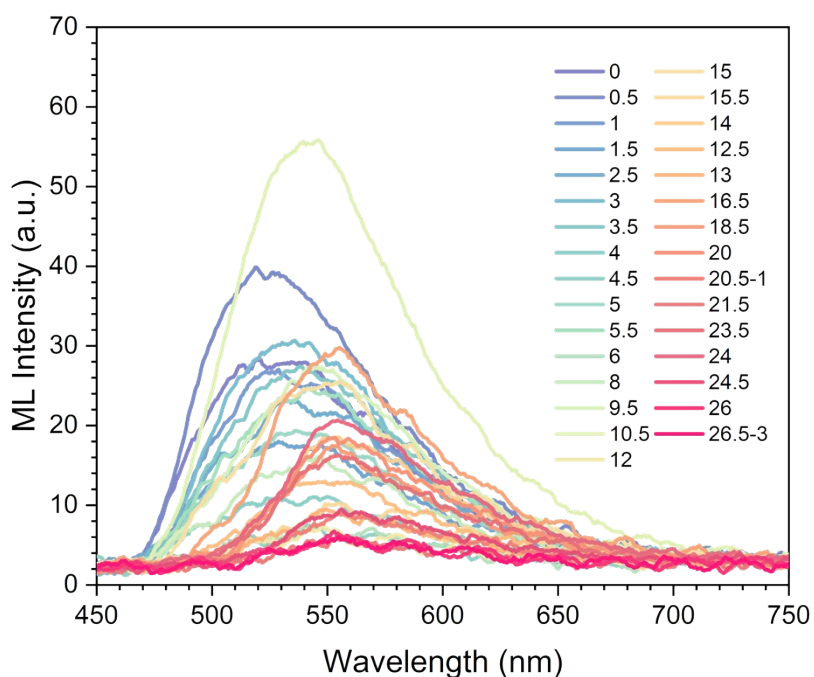


**Figure S3.** ML spectra of PTZ-2BP under continuous mechanical stimulus within 30 s.

**Table S2.** ML wavelength of PTZ-2BP under continuous mechanical grinding within 30 s.

Grinding time (s)	$\lambda_{ML}$ (nm)	Grinding time (s)	$\lambda_{ML}$ (nm)
0.0	520	12.5	549
0.5	520	13.0	550
1.0	528	14.0	555
1.5	529	15.0	555
2.5	530	15.5	555
3.0	536	16.5	555
3.5	538	18.5	554
4.0	545	20.0	553
4.5	541	20.5	556
5.0	537	21.5	554
5.5	542	23.5	555
6.0	542	24.0	555
8.0	547	24.5	556
9.5	544	26.0	553
10.5	546	26.5	555
12.0	548	\	\

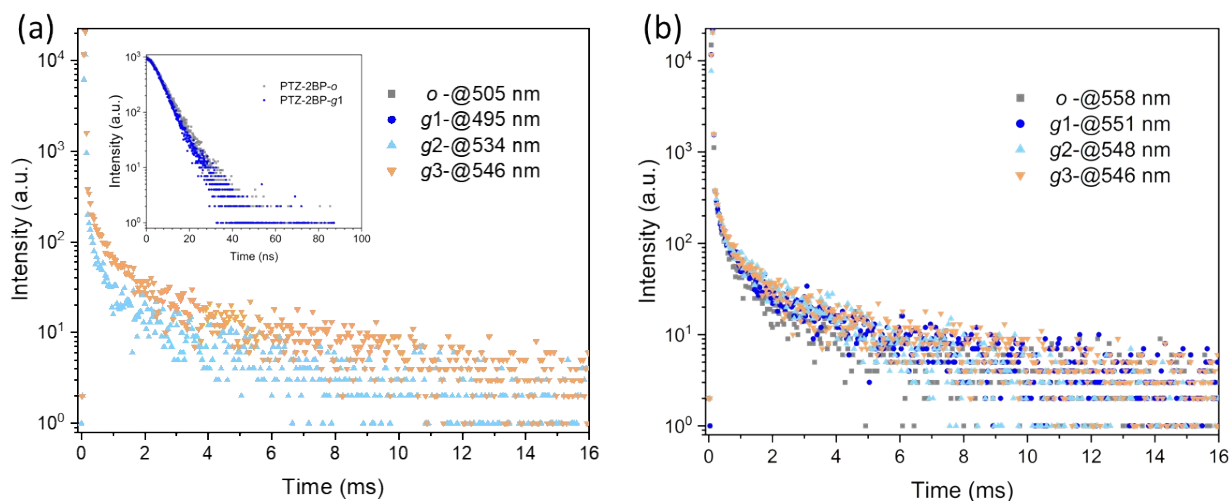
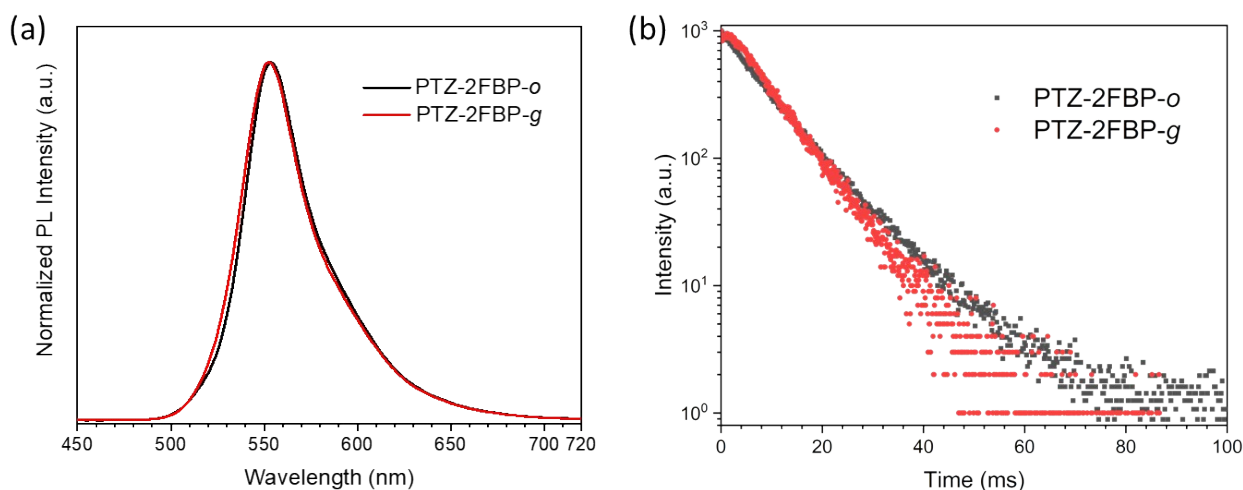


**Figure S4.** The (a) PL decay and (b) long-lived PL decay of PTZ-2BP in different states. (*o*: the as-

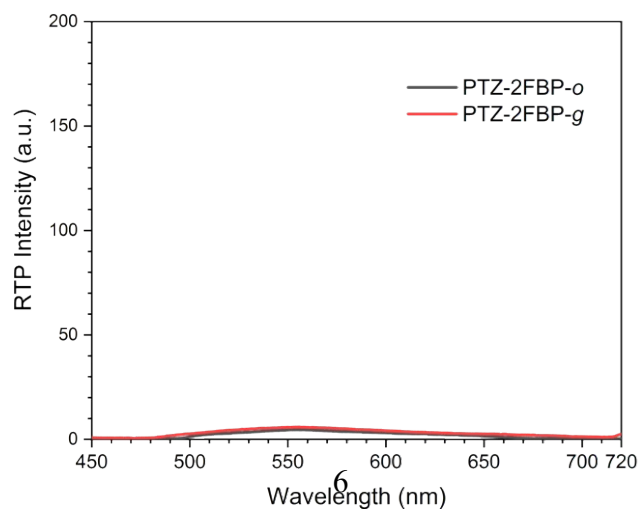


prepared state; *g*1: ground state of *o*; *g*2; ground state of *g*1; *g*3: ground state of *g*2.)

**Figure S5.** (a) Normalized PL spectra of PTZ-2FBP in original (-*o*) and ground (-*g*) states; (b) PL decay of PTZ-2FBP in original (-*o*) and ground (-*g*) states.

**Figure S6.** The delayed PL spectra of PTZ-2FBP in original (-*o*) and ground (-*g*) states.

**Table S3.** Optical properties of PTZ-2FBP in *o* and *g* state.



state	$\lambda_{\text{PL}}^{\text{a}}$ (nm)	$\tau_{\text{PL}}^{\text{a}}$ (ns)	$\Phi^{\text{b}}$ (%)
<i>o</i>	<b>555</b>	<b>10.22</b>	<b>49.47</b>
<i>g</i>	<b>552</b>	<b>8.13</b>	<b>32.99</b>

<sup>a</sup> The maximum emission wavelength ( $\lambda_{\text{PL}}$ ) of photoluminescence and corresponding lifetime ( $\tau_{\text{PL}}$ ). <sup>b</sup> The photoluminescence quantum yield ( $\Phi$ ). (All the data were collected at room temperature in air.)

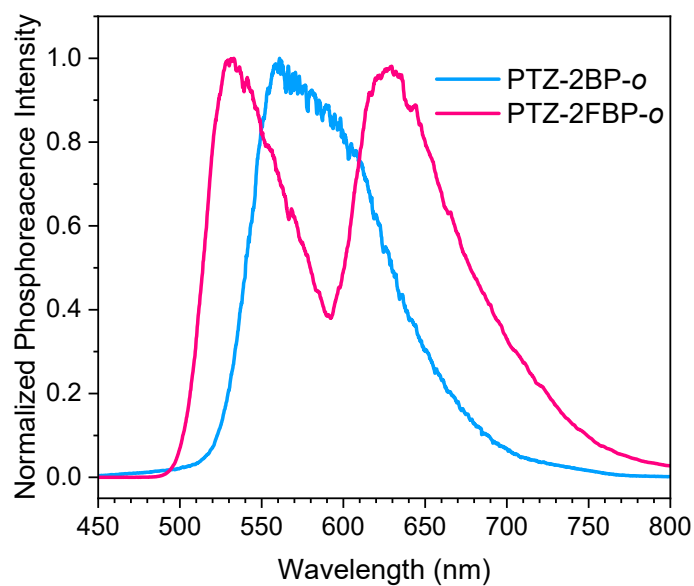


**Figure S7.** The phosphorescence spectra of PTZ-2BP and PTZ-2FBP in the as-prepared state at 77 K.

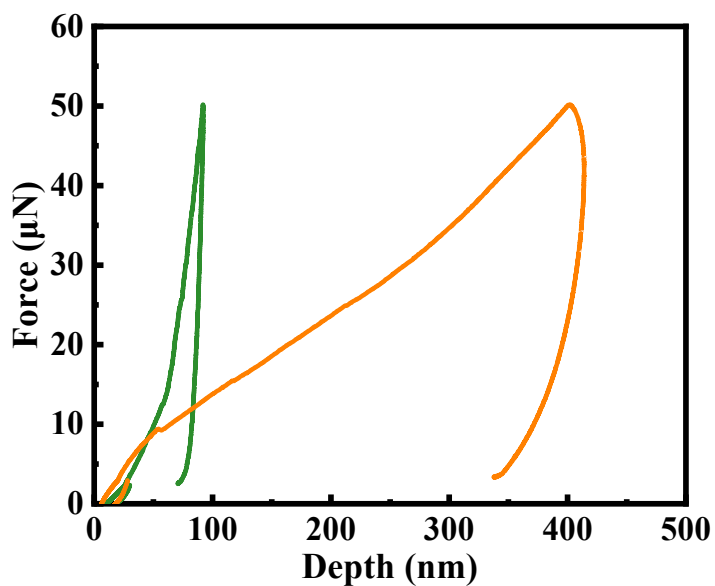


**Figure S8.** The nanoindentation test of a typical load versus displacement (P-h) curve

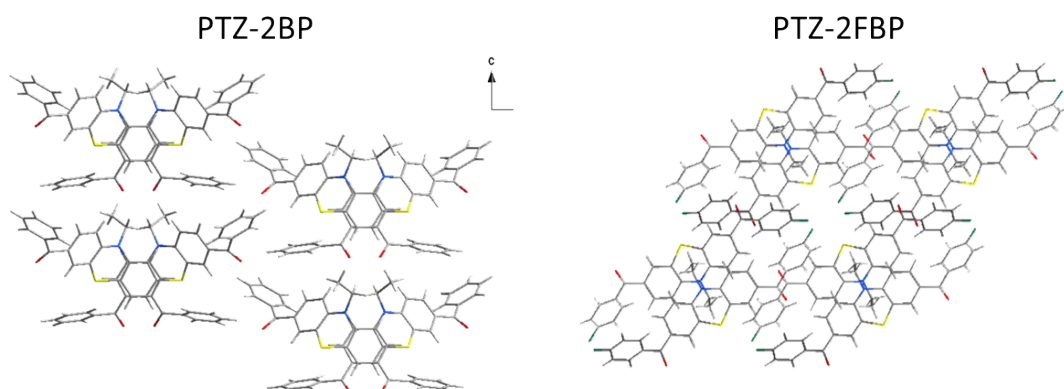


**Figure S9.** The molecular packing in the crystals of PTZ-2BP and PTZ-2FBP.

**Table S4.** Structure data of PTZ-2BP and PTZ-2FBP crystals.

Name	PTZ-2BP	PTZ-2FBP
Empirical formula	C <sub>28</sub> H <sub>21</sub> NO <sub>2</sub> S	C <sub>28</sub> H <sub>19</sub> F <sub>2</sub> NO <sub>2</sub> S
Wavelength (Å)	1.54184	0.71073
Crystal system	orthorhombic	triclinic
Space group	<i>Pna</i> 2 <sub>1</sub> (33)	<i>P</i> -1 (2)
	Non-centrosymmetric	Centrosymmetric
Unit cell angles (°)	$\alpha = 90$	$\alpha = 86.808(1)$
	$\beta = 90$	$\beta = 84.321(1)$
	$\gamma = 90$	$\gamma = 80.408(1)$
Unit cell length (Å)	$a = 7.287(4)$	$a = 8.356(4)$
	$b = 31.403(13)$	$b = 12.466(6)$
	$c = 9.407(4)$	$c = 20.999(8)$
Unit cell volume (Å <sup>3</sup> )	2153.02(18)	2144.82(17)
Z	4	4
Density (g/cm <sup>3</sup> )	1.344	1.460
F(000)	912.0	976.0
CCDC number	2391558	2391557



**Table S5.** Summarization of intermolecular interactions in the molecular dimer derived from the unit cell of PTZ-2BP.

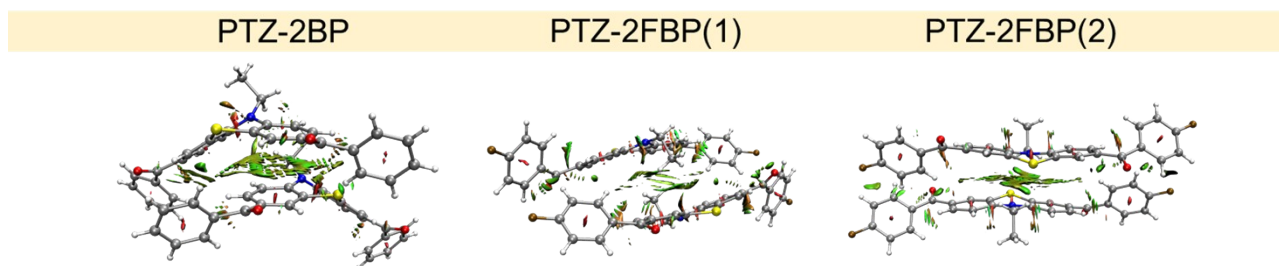
<b>Dimer of PTZ-2BP</b>			
Position of interaction	Type of Interaction	d /Å	Number(2)
1	$\pi \dots \pi$	3.654	1
2	$\pi \dots \pi$	3.879	1
	Type of Interaction	d /Å	Number(8)
1	C-H... $\pi$	<b>2.998</b>	1
2	C-H... $\pi$	3.352	1
3	C-H... $\pi$	3.409	1
4	C-H... $\pi$	3.467	1
5	C-H... $\pi$	3.744	1
6	C-H... $\pi$	3.855	1
7	C-H... $\pi$	3.919	1
8	C-H... $\pi$	3.934	1
	Type of Interaction	d /Å	Number(3)
1	C-H...N	3.301	1
2	C-H...N	3.524	1
3	C-H...N	3.800	1
	Type of Interaction	d /Å <sup>a</sup>	Number(5)
1	C-H...S	<b>2.763</b>	1
2	C-H...S	3.281	1
3	C-H...S	3.449	1
4	C-H...S	3.529	1
5	C-H...S	3.924	1
	Type of Interaction	d /Å <sup>a</sup>	Number(1)
1	C-H...O	<b>2.985</b>	1

**Table S6.** Summarization of intermolecular interactions in the molecular dimer 1 derived from the unit cell of PTZ-2FBP.

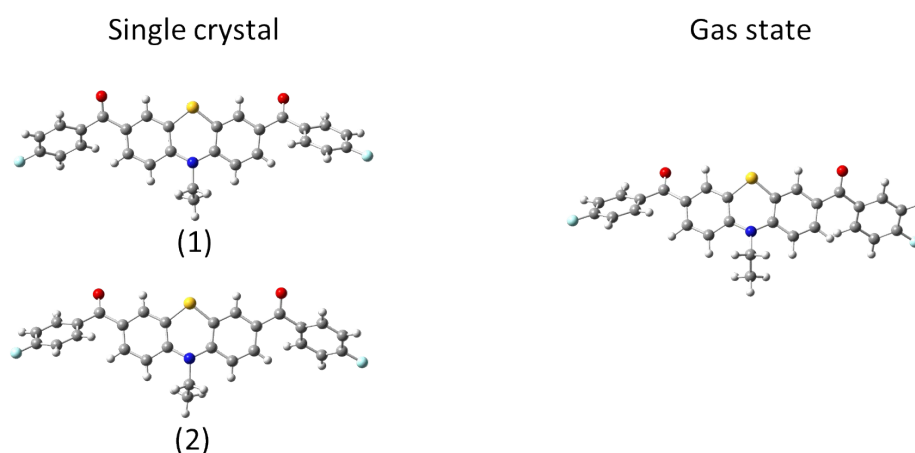
<b>Dimer-1 of PTZ-2FBP</b>				
Position of interaction	Type of Interaction	d /Å	Number(16)	
	1 C-H... $\pi$	<b>2.894</b>	2	
Alkyl chain	2 C-H... $\pi$	<b>2.944</b>	2	
Alkyl chain	3 C-H... $\pi$	2.949	2	
Alkyl chain	4 C-H... $\pi$	3.287	2	
Alkyl chain	5 C-H... $\pi$	3.602	2	
Alkyl chain	6 C-H... $\pi$	3.616	2	
Alkyl chain	7 C-H... $\pi$	3.809	2	
Alkyl chain	8 C-H... $\pi$	3.813	2	
	Type of Interaction	d /Å	Number(4)	
Alkyl chain	1 C-H...N	3.237	2	
Alkyl chain	2 C-H...N	3.493	2	
	Type of Interaction	d /Å <sup>a</sup>	Number(4)	
Alkyl chain	1 C-H...S	3.724	2	
Alkyl chain	2 C-H...S	3.784	2	
	Type of Interaction	d /Å <sup>a</sup>	Number(2)	
	1 C-H...F	3.145	2	

**Table S7.** Summarization of intermolecular interactions in the molecular dimer 2 derived from the unit cell of PTZ-2FBP.

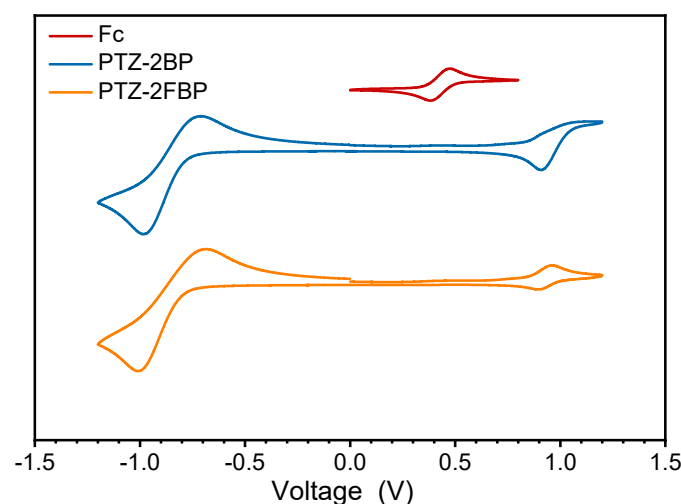
<b>Dimer-2 of PTZ-2FBP</b>				
Position of interaction	Type of Interaction	d /Å	Number(12)	
Alkyl chain	1 C-H... $\pi$	<b>2.906</b>	2	
	2 C-H... $\pi$	3.029	2	
Alkyl chain	3 C-H... $\pi$	3.267	2	
Alkyl chain	4 C-H... $\pi$	3.404	2	
Alkyl chain	5 C-H... $\pi$	3.932	2	
	6 C-H... $\pi$	3.997	2	
	Type of Interaction	d /Å	Number(6)	
Alkyl chain	1 C-H...N	3.168	2	
Alkyl chain	2 C-H...N	3.635	2	
	3 C-H...N	3.950	2	
	Type of Interaction	d /Å	Number(4)	
Alkyl chain	1 C-H...S	3.161	2	
Alkyl chain	2 C-H...S	3.616	2	
	Type of Interaction	d /Å	Number(4)	
	1 C-H...F	3.234	2	
	2 C-H...F	3.978	2	



**Figure S10.** The calculated intramolecular noncovalent interactions (NCI) based on reduced density gradient (RDG) in the molecular dimer derived from the unit cell of PTZ-2BP or PTZ-2FBP.



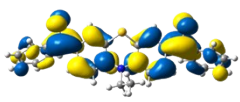
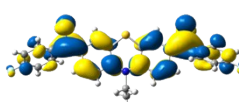
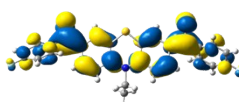
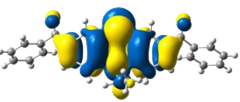
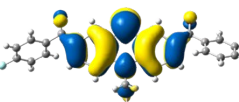
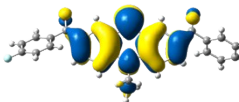
**Figure S11.** The calculated conformations based on PTZ-2FBP (left: from single crystal; right: from theoretical calculation).



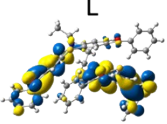
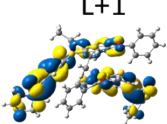
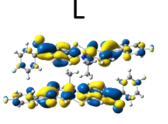
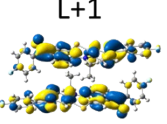
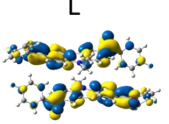
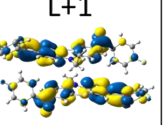
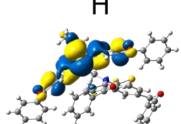
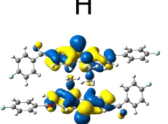
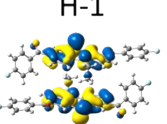
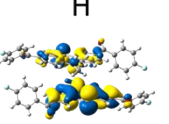
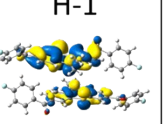
**Figure S12.** The electrochemical cyclic voltammetry curves of PTZ-2BP and PTZ-2FBP.

Cyclic voltammetry (CV) measurements were carried out to investigate the electrochemical properties of the two compounds. The highest occupied molecular orbital (HOMO) energy levels were estimated from the onset oxidation potentials, following the equation:  $\text{HOMO} = -(4.8 + E_{\text{ox}} - E_{(\text{Fc}/\text{Fc}^+)})$  eV, while the lowest unoccupied molecular orbital (LUMO) energy levels were determined by combining the optical band-gap energies (estimated from the onset wavelengths of the UV absorptions) and HOMO

values. As shown in Fig. S12, the HOMO values of PTZ-2BP and PTZ-2FBP in CH<sub>2</sub>Cl<sub>2</sub> solution (single molecule) are calculated to be -5.22 eV and -5.23 eV, respectively. And their corresponding LUMO energy levels in CH<sub>2</sub>Cl<sub>2</sub> solution (single molecule) were calculated to be -2.60 eV and -2.61 eV, respectively. These results indicate similar electronic properties in single molecule of PTZ-2BP and PTZ-2FBP.

Monomer	PTZ-2BP	PTZ-2FBP (1)	PTZ-2FBP (2)
LUMO	 -1.67 eV	 -1.90 eV	 -1.89 eV
HOMO	 -5.39 eV	 -5.22 eV	 -5.22 eV
$\Delta E_g$	3.72 eV	3.32 eV	3.33 eV

**Figure S13.** The HOMO and LUMO of the single molecules in the PTZ-2BP and PTZ-2FBP calculated at B3LYP/6-31G(d, p) level.

Dimer	PTZ-2BP	PTZ-2FBP (1)	PTZ-2FBP (2)
LUMO	  -1.74 eV      -1.72 eV	  -2.11 eV      -2.08 eV	  -2.11 eV      -2.09 eV
HOMO	 -5.39 eV	  -5.40 eV      -5.43 eV	  -5.45 eV      -5.45 eV
$\Delta E_g$	3.65 eV	3.29 eV	3.34 eV

**Figure S14.** The HOMO and LUMO of the dimers in the PTZ-2BP and PTZ-2FBP calculated at B3LYP/6-31G(d, p) level.

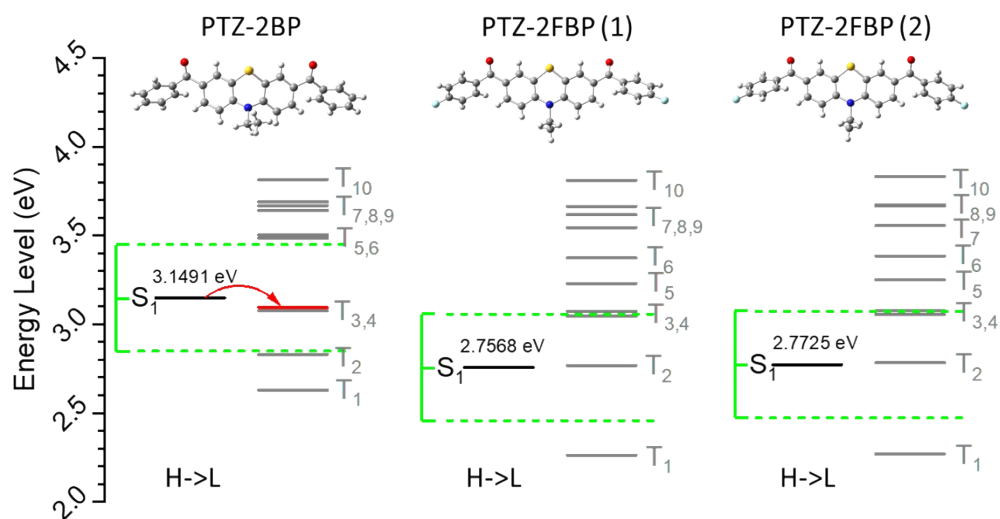


**Figure S15.** The lowest singlet ( $S_1$ ) and triplet ( $T_n$ ) states of a PTZ-2BP monomer and two PTZ-2FBP monomers, respectively obtained by TD-DFT calculations based on the single crystal structure data of PTZ-2BP and PTZ-2FBP.

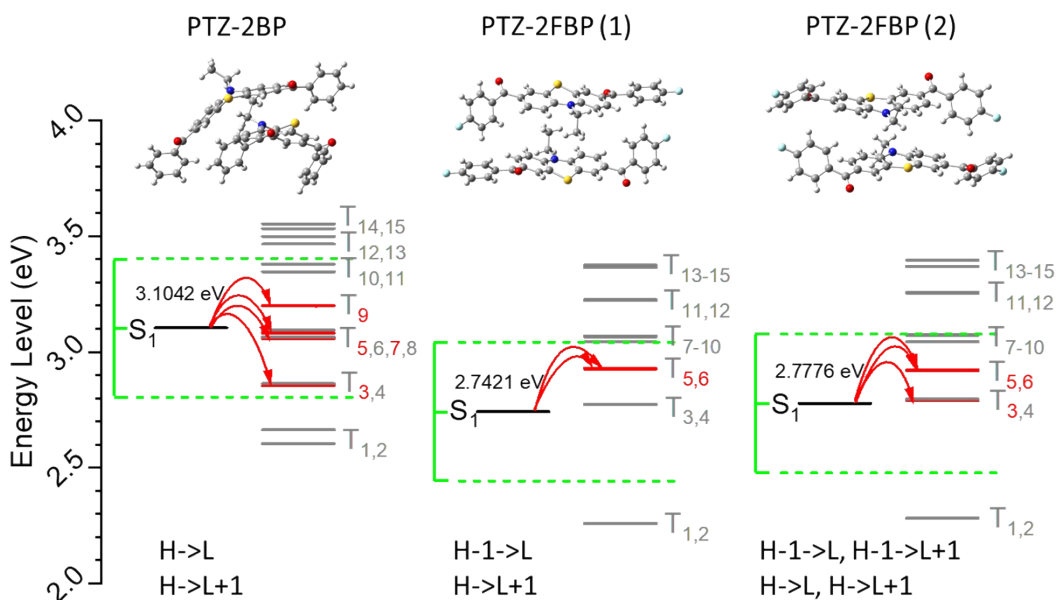


**Figure S16.** The lowest singlet ( $S_1$ ) and triplet ( $T_n$ ) states of a PTZ-2BP dimer and two PTZ-2FBP dimers, respectively obtained by TD-DFT calculations based on the single crystal structure data of PTZ-2BP and PTZ-2FBP.

**Table S8.** Singlet and triplet excited state transition configurations of PTZ-2BP monomer and PTZ-2FBP monomers revealed by TD-DFT calculations.

Monomer-PTZ-2BP (eV)	Monomer-PTZ-2FBP (1) (eV)	Monomer-PTZ-2FBP (2) (eV)
T1: 2.6293	T1: 2.2624	T1: 2.2692
T2: 2.8303	S1: 2.7568 H ->L (96.7%)	S1: 2.7725 H ->L (96.7%)
T3: 3.0750 H ->L (3.1%)	T2: 2.7682	T2: 2.7824
T4: 3.0941	T3: 3.0451	T3: 3.0552
S1: 3.1491 H ->L ( 96.4%)	T4: 3.0732	T4: 3.0753
T5: 3.4854	T5: 3.2299	T5: 3.2501
T6: 3.5038	T6: 3.3739	T6: 3.3851
T7: 3.6412	T7: 3.5451	T7: 3.5561
T8: 3.6682	T8: 3.6180	T8: 3.6655
T9: 3.6900	T9: 3.6633	T9: 3.6736
T10: 3.8153	T10: 3.8102	T10: 3.8322
T11: 4.1667	T11: 4.0085	T11: 4.0354
T12: 4.1862	T12: 4.1911	T12: 4.2004
T13: 4.2750	T13: 4.1960	T13: 4.2140
T14: 4.2830	T14: 4.2943	T14: 4.2891
T15: 4.3533	T15: 4.3114	T15: 4.3017

**Table S9.** Singlet and triplet excited state transition configurations of PTZ-2BP dimer and PTZ-2FBP dimers revealed by TD-DFT calculations.

Dimer-PTZ-2BP (eV)	Dimer-PTZ-2FBP (1) (eV)	Dimer-PTZ-2FBP (2) (eV)
T1: 2.6037	T1: 2.2572	T1: 2.2808
T2: 2.6636	T2: 2.2588	T2: 2.2829
T3: 2.8537 H ->L (3.4%)	S1: 2.7421 H-1 ->L (51.3%) H ->L+1 (45.6%)	S1: 2.7776 H-1 ->L (52.1%) H-1 ->L+1 (3.3%) H ->L (4.2%) H ->L+1 (37.2%)
T4: 2.8634	T3: 2.7737	T3: 2.7903 H-1 ->L+1 (2.5%) H ->L (2.6%)
T5: 3.0584 H ->L(2.4%) H ->L+1 (2.3%)	T4: 2.7742	T4: 2.7957
T6: 3.0655	T5: 2.9270 H-1 ->L (39.7%) H ->L+1 (41.6%)	T5: 2.9194 H-1 ->L (28.9%) H ->L (20.0%) H ->L+1 (50.4%)
T7: 3.0818 H ->L (3.2%)	T6: 2.9286 H-1 ->L (8.8%) H ->L+1 (9.3%)	T6: 2.9220 H-1 ->L (15.7%) H-1 ->L+1 (49.9%) H ->L (27.7%)
T8: 3.0947	T7: 3.0425	T7: 3.0447
S1: 3.1042 H ->L (25.5%) H ->L+1 (67.8%)	T8: 3.0435	T8: 3.0450
T9: 3.1998 H ->L (39.4%) H ->L+1 (23.9%)	T9: 3.0662	T9: 3.0724
T10: 3.3467	T10: 3.0687	T10: 3.0745
T11: 3.3803	T11: 3.2222	T11: 3.2550
T12: 3.4660	T12: 3.2263	T12: 3.2579
T13: 3.4993	T13: 3.3656	T13: 3.3683
T14: 3.5333	T14: 3.3680	T14: 3.3704
T15: 3.5535	T15: 3.3752	T15: 3.3970

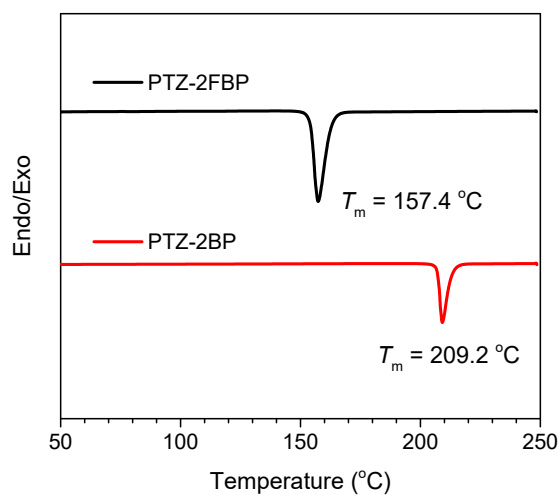


**Figure S17.** The Differential Scanning Calorimetry (DSC) curves of PTZ-2BP and PTZ-2FBP. ( $T_m$ : melting temperature).

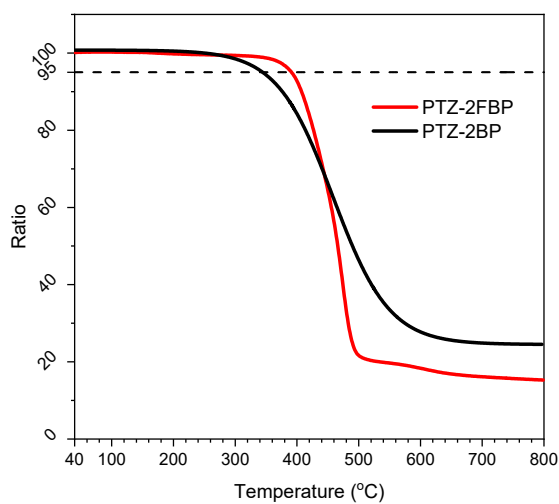


**Figure S18.** The Thermogravimetric analysis (TGA) curves of PTZ-2BP and PTZ-2FBP.

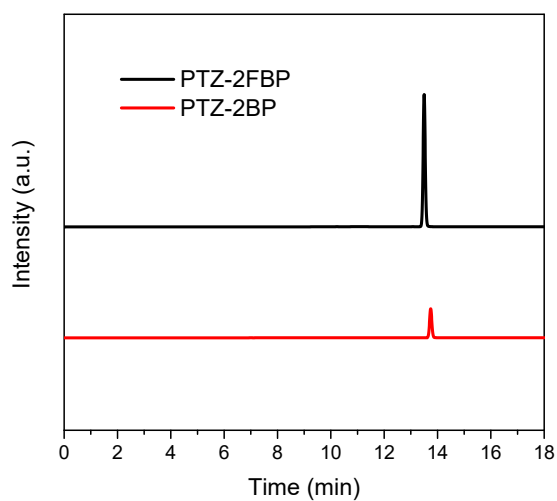
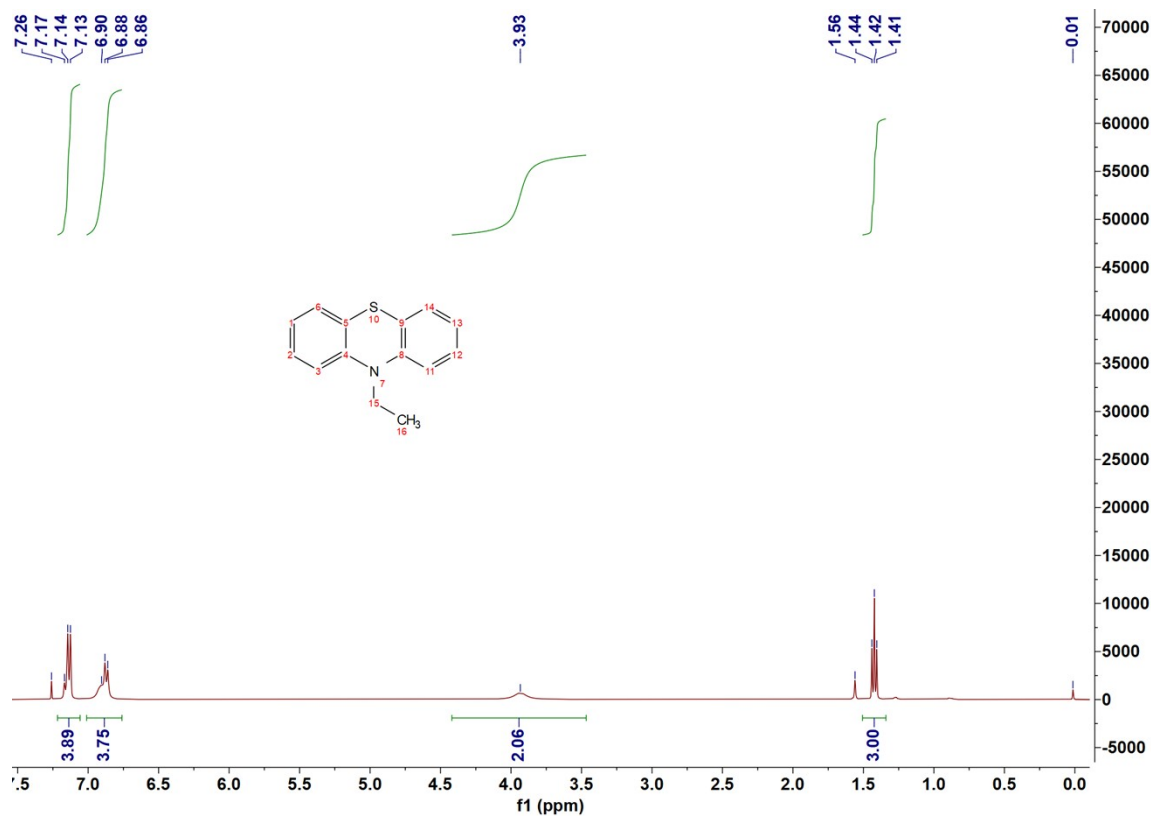


**Figure S19.** The High Performance Liquid Chromatography (HPLC) of PTZ-2BP and PTZ-2FBP.

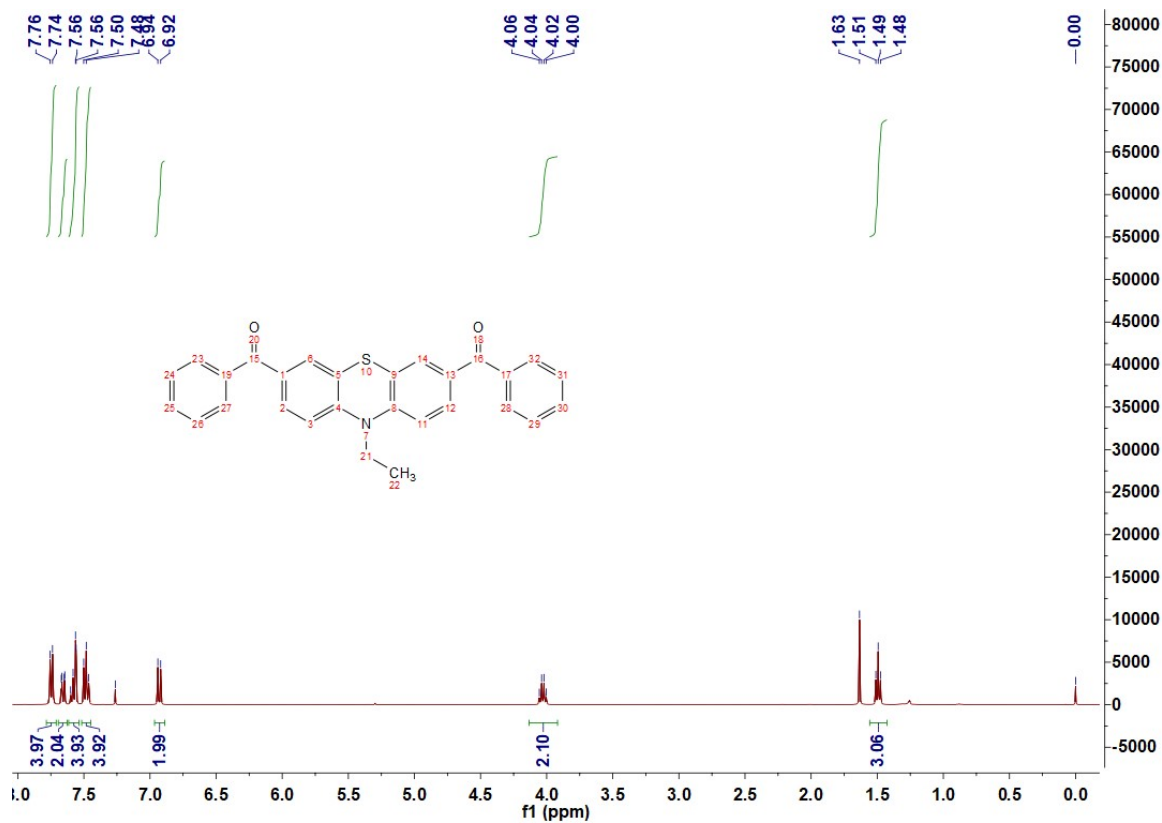




#### 4. Structure Information

**Figure S20.**  $^1\text{H}$  NMR spectrum of compound 2 conducted in  $\text{CDCl}_3$ .

**Figure S21.**  $^1\text{H}$  NMR spectrum of PTZ-2BP conducted in  $\text{CDCl}_3$ .



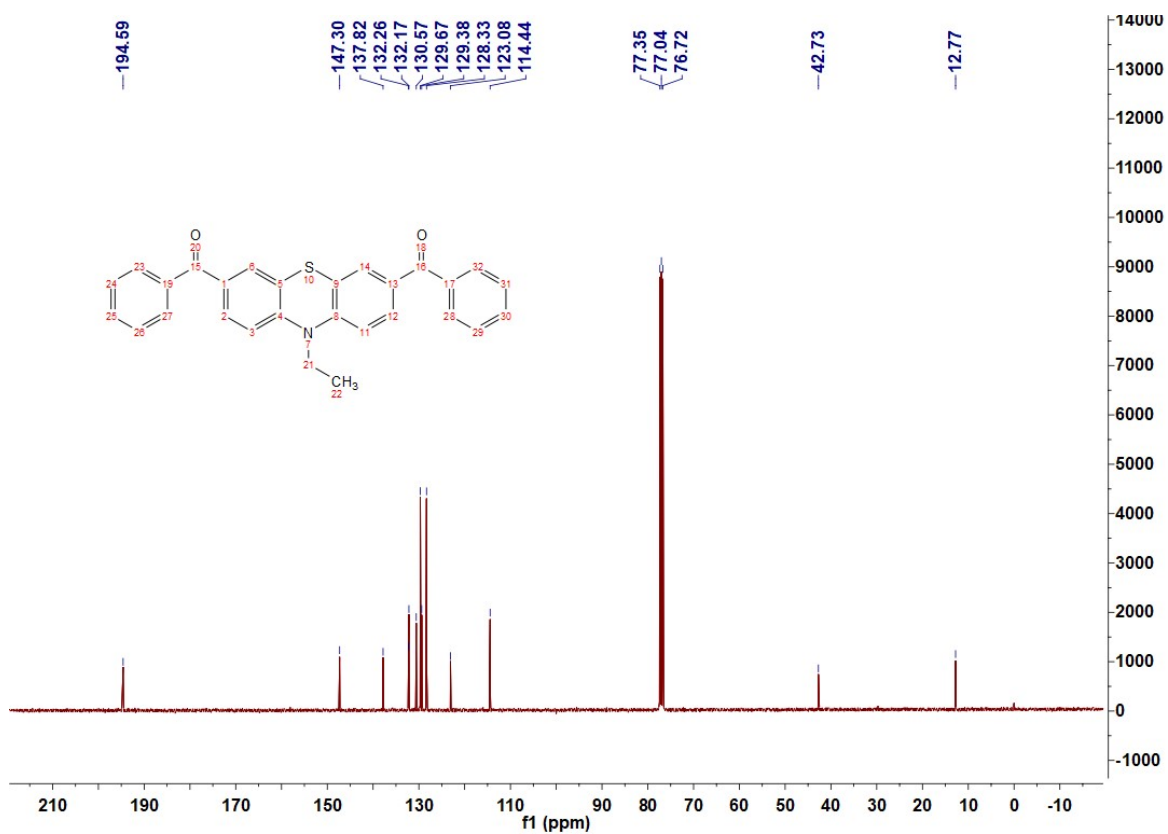


**Figure S22.** <sup>13</sup>C NMR spectrum of PTZ-2BP conducted in CDCl<sub>3</sub>.

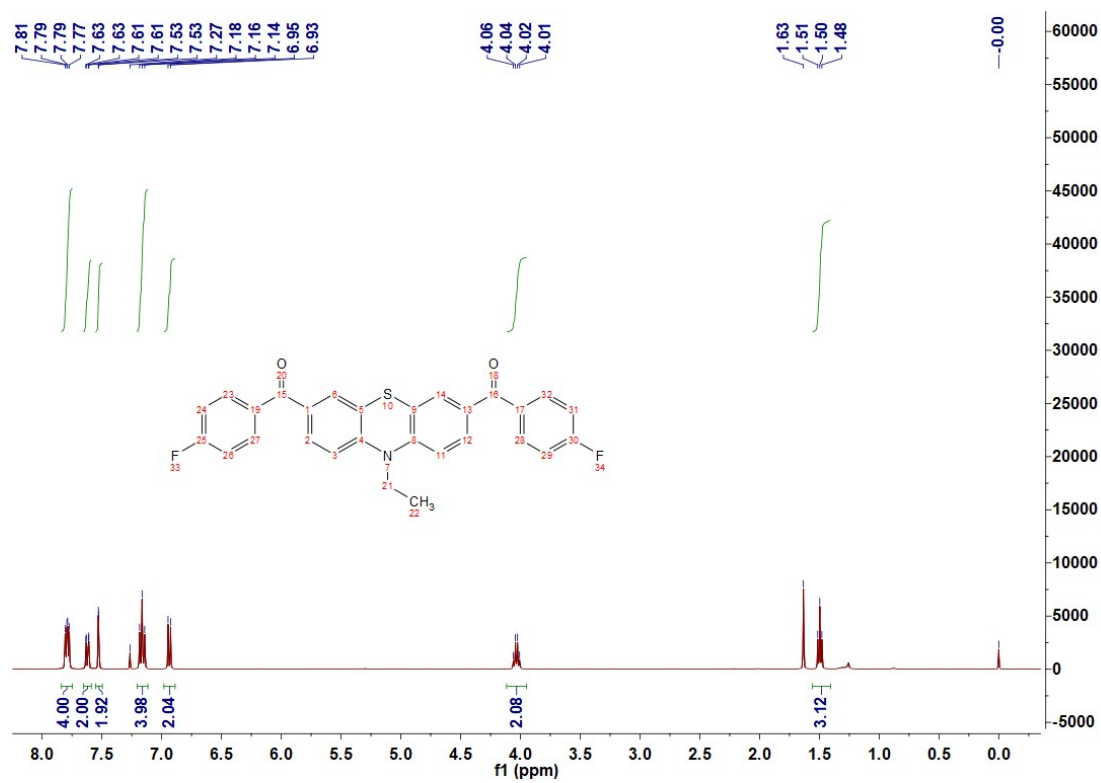


**Figure S23.** <sup>1</sup>H NMR spectrum of PTZ-2FBP conducted in CDCl<sub>3</sub>.

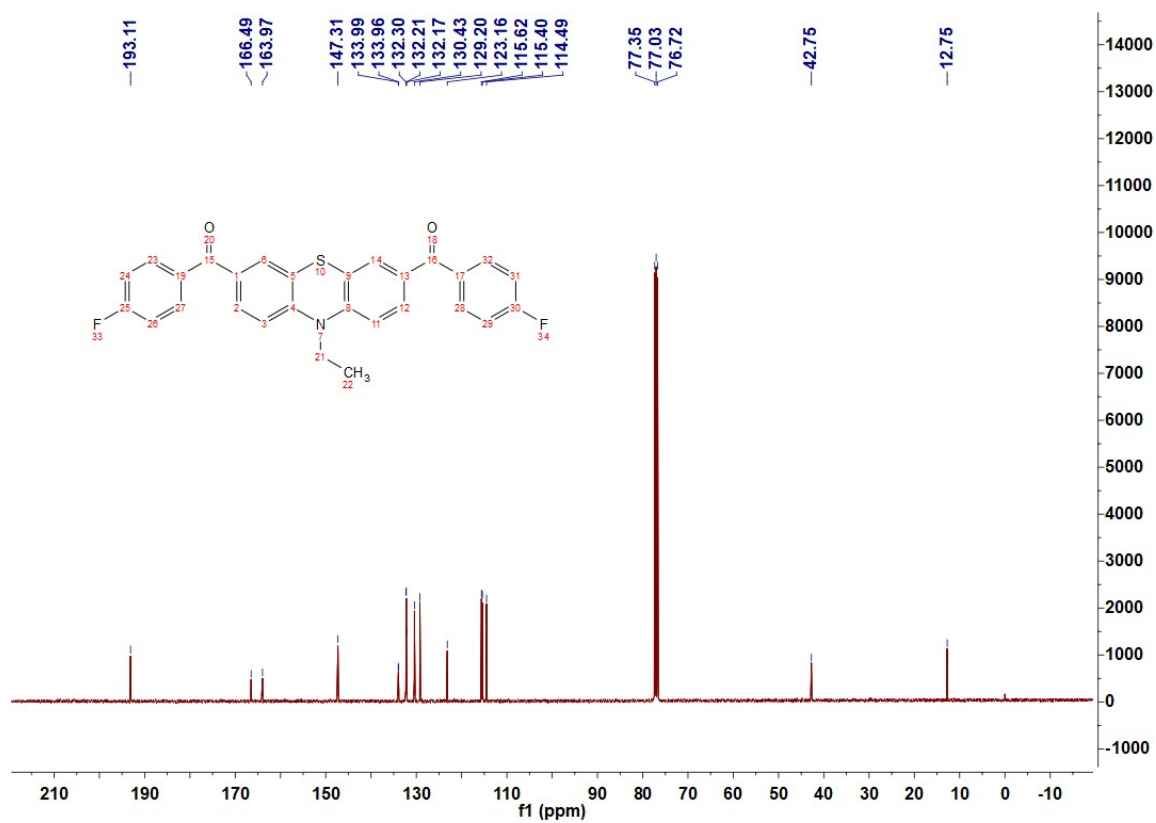


**Figure S24.** <sup>13</sup>C NMR spectrum of PTZ-2FBP conducted in CDCl<sub>3</sub>